The Cryosphere, 9, 1223–1227, 2015
www.the-cryosphere.net/9/1223/2015/
doi:10.5194/tc-9-1223-2015

The Cryosphere
Open Access

Brief Communication: Newly developing rift in Larsen C Ice Shelf presents significant risk to stability

D. Jansen[1], A. J. Luckman[2], A. Cook[2], S. Bevan[2], B. Kulessa[2], B. Hubbard[3], and P. R. Holland[4]

[1]Alfred-Wegener-Institut Helmholtz-Zentrum für Polar- und Meeresforschung, Bremerhaven, Germany
[2]Department of Geography, College of Science, Swansea University, Swansea, UK
[3]Centre for Glaciology, Institute for Geography and Earth Sciences, Aberystwyth University, Aberystwyth, UK
[4]British Antarctic Survey, High Cross, Cambridge, UK

Correspondence to: D. Jansen (daniela.jansen@awi.de)

Received: 5 February 2015 – Published in The Cryosphere Discuss.: 11 February 2015
Revised: 19 May 2015 – Accepted: 23 May 2015 – Published: 15 June 2015

Abstract. An established rift in the Larsen C Ice Shelf, formerly constrained by a suture zone containing marine ice, grew rapidly during 2014 and is likely in the near future to generate the largest calving event since the 1980s and result in a new minimum area for the ice shelf. Here we investigate the recent development of the rift, quantify the projected calving event and, using a numerical model, assess its likely impact on ice shelf stability. We find that the ice front is at risk of becoming unstable when the anticipated calving event occurs.

1 Introduction

The Larsen C Ice Shelf is the most northerly of the remaining major Antarctic Peninsula ice shelves and is vulnerable to changes in both ocean and atmospheric forcing (Holland et al., 2015). It is the largest ice shelf in the region and its loss would lead to a significant drawdown of ice from the Antarctic Peninsula Ice Sheet (APIS). There have been observations of widespread thinning (Shepherd et al., 2003; Pritchard et al., 2012; Holland et al., 2015), melt ponding in the northern inlets (Holland et al., 2011; Luckman et al., 2014), and a speed-up in ice flow (Khazendar et al., 2011), all processes which have been linked to former ice shelf collapses (e.g. van den Broeke, 2005). Previous studies have highlighted the vulnerability of Larsen C Ice Shelf to specific potential changes in its geometry including a retreat from the Bawden Ice Rise (Kulessa et al., 2014; McGrath et al., 2014; Holland et al., 2015) and Gipps Ice Rise (Borstad et al., 2013). Rift tips in the latter area have been observed to align as they terminate at a confluence of flow units within the shelf. Several studies have provided evidence for marine ice in these *suture zones* (Holland et al., 2009; Jansen et al., 2013; Kulessa et al., 2014; McGrath et al., 2014). The relatively warm, and thus soft, marine ice has been found to act as a weak coupling between flow units with different flow velocities. It has been concluded that this ice inhibits the propagation of rifts because it can accommodate strain in the ice without fracturing further (Holland et al., 2009; Jansen et al., 2013; Kulessa et al., 2014).

In a change from the usual pattern, a northward-propagating rift from Gipps Ice Rise has recently penetrated through the suture zone and is now more than halfway towards calving off a large section of the ice shelf (Figs. 1 and 2). The rate of propagation of this rift accelerated during 2014. When the next major calving event occurs, the Larsen C Ice Shelf is likely to lose around 10 % of its area to reach a new minimum both in terms of direct observations, and possibly since the last interglacial period (Hodgson et al., 2006).

Here, using satellite imagery and numerical modelling, we document the development of the rift over recent years, predict the area of ice that will be lost, and test the likely impact of this future calving event on ice shelf stability.

Published by Copernicus Publications on behalf of the European Geosciences Union.

2 Methods

2.1 Satellite observations

We use data from NASA MODIS at a pixel size of 250 m (red band) from the near-real-time archive (http://lance-modis.eosdis.nasa.gov/cgi-bin/imagery/realtime.cgi) to monitor the general propagation of the rift and to explore its likely future path (Fig. 1). These data, however, did not provide sufficiently high spatial resolution to measure the rift tip position with satisfactory precision. Using Landsat data at high spatial resolution (15 m, panchromatic) from the NASA archive (http://earthexplorer.usgs.gov/), we measure in detail the rift's recent propagation (Fig. 2). Growth of the rift is assessed by digitizing the position of the rift tip in all Landsat images unobscured by cloud between November 2010 and January 2015 working within the polar stereographic map projection in which the data were provided. The start of this sequence is chosen to show normal behaviour of the rift over 3 years before its more rapid propagation in 2014. Between January 2015 and the final paper submission, no additional images showed notable further propagation. Rift length is presented relative to the position in November 2010 prior to the breach of the Joerg Peninsula suture zone. Rift width is measured at the November 2010 rift tip position. These satellite data are subject to variable cloud conditions and solar illumination, the impact of which we minimize by optimizing brightness and contrast in each image separately. Nevertheless, measurements of rift tip position and width are potentially subject to error of up to a few tens of metres. A table listing all Landsat images used for this study as well as the measured rift lengths and widths can be found in the Supplement.

To investigate a range of possible outcomes from the proposed calving event, we present two scenarios for the rift trajectory based on its current orientation and direction of propagation, and on visual inspection of MODIS data (Fig. 1). Surface features in these data indicate the scale and orientation of existing weaknesses (e.g. basal crevasses) along which the rift might be expected to preferentially propagate (Luckman et al., 2012). In Scenario I the rift approaches the calving front by the shortest route via existing weaknesses, and so would result in a reasonable minimum estimate for the calved area. In Scenario II the rift continues along its current trajectory for a further 80 km before approaching the ice front. The hypothetical turning point in this scenario is chosen to smoothly continue the orientation of the ice front where the rift will meet it (Fig. 1), and imitates the pattern of calving of a large iceberg in 2008. We present these scenarios as reasonable possibilities for which to test the impact of a calving event, rather than a range for the projected calved area. The eventual calving may be within the range we test, or may be more extreme still.

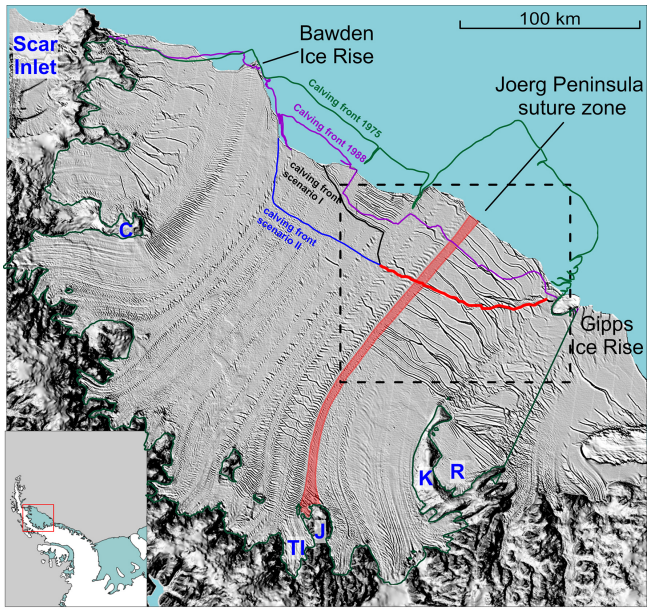

Figure 1. Overview of the Larsen C Ice Shelf in late 2014 showing the contemporary location of the developing rift (red line), and a selection of previous and predicted future calving fronts. Background image is MODIS Aqua, 3 December 2014 for the ice shelf and a shaded relief digital elevation model of the Antarctic Peninsula mountains: Cook et al. (2012). Geographic features of interest are marked (TI – Trail Inlet, K – Kenyon Peninsula, R – Revelle Inlet, J – Joerg Peninsula, C – Churchill Peninsula) and the dashed box shows the extent of Fig. 2. The highlighted flow line indicates the location of the Joerg Peninsula suture zone.

2.2 Numerical modelling

To determine the influence of the potential calving event on the future stability of the Larsen C Ice Shelf we use a numerical ice shelf model, previously applied to the Larsen B (Sandhäger et al., 2005) and the Larsen C ice shelves (Jansen et al., 2010, 2013; Kulessa et al., 2014). This finite difference model is based on the continuum mechanical equations of ice shelf flow. Friction at the ice shelf base as well as vertical shear strain due to bending is neglected. Thus horizontal flow velocities are vertically invariant and the flow field is two-dimensional. In the vertical dimension the model domain is divided into 13 levels, scaled by ice thickness, to allow for a realistic vertical temperature profile, influencing the vertically integrated flow parameter.

Simulations are carried out on a 2.5 km grid varying only the position of the ice shelf calving margin between the present ice front position and rift Scenarios I and II. The model we apply is a steady-state mode which assumes that the ice shelf is not in transition from one geometry to another. It is important, therefore, to investigate the present stress field at the predicted calving margin as well as the new stress field at the predicted calving margin under the new geometries. These two states represent the stress field imme-

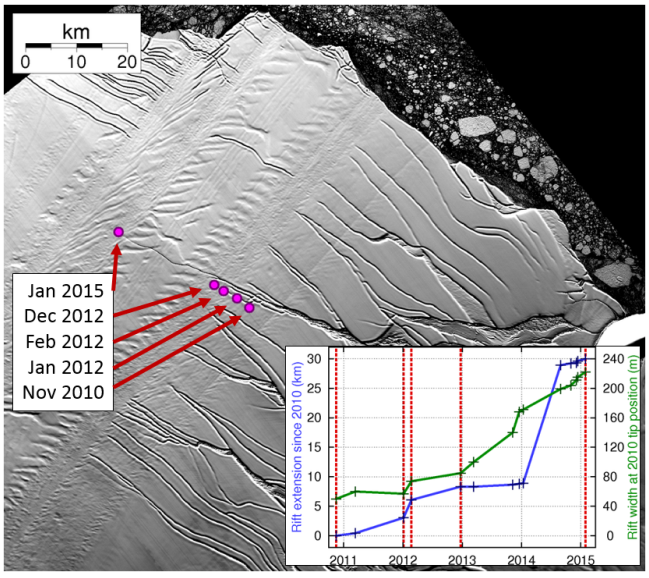

Figure 2. Analysis of rift propagation using Landsat data. Background image, in which the rift is visible, is from 4 December 2014. Inset graph shows the development of rift length with respect to the 2010 tip position, and rift width at the 2010 tip position, measured from all available Landsat images (crosses; 15 in total). The line joining data points illustrates only the mean propagation rate between observations. Actual propagation of the rift may be sporadic and true propagation rates cannot be known without regular frequent observations, which are not available. Circles and labels on the map, and dotted red lines on the graph, show the positions of notable stages of rift development.

diately after calving, and the stress field towards which the shelf will develop in time through the process of the velocity field adapting to the new geometry (assuming no immediate further calving). The two stress fields may be different, and may indicate increasing or decreasing stability under the new geometries.

3 Results

3.1 Rift evolution and possible calving scenarios

The rift first propagated into the Joerg Peninsula suture zone in 2012 and progressed during 2013 into a region which previously appeared to resist transverse fractures (Fig. 2). The rate of rift propagation increased sometime between January and August 2014, crossing the entire Trail Inlet flow unit (~ 20 km) in just 8 months. We do not have observations within this time period so we cannot say whether the rift propagation during this time period was uniform or was very rapid for only a short part of it. Between August 2014 and late January 2015, the rift length increased further about 1.25 km, propagating into the next suture zone. From the start of our measurements the width of the rift at the 2010 rift tip position has increased at a more uniform rate than the length, and is still growing at a rate of $\sim 40\,\mathrm{m\,yr^{-1}}$ (Fig. 2).

The area of Larsen C Ice Shelf after the proposed calving event will be 4600 $\mathrm{km^2}$ less than at present for Scenario I, and 6400 $\mathrm{km^2}$ less for Scenario II (Fig. 1). This amounts to potential area losses of 9 and 12 % respectively.

The last large calving event of the Larsen Ice Shelf occurred in 1986, where several large tabular icebergs calved from its southern front. The location of the front after the calving was approximately 18 km upstream of its current position (Fig. 1, see also Cook and Vaughan, 2010). The shape of the calving front in 1988 indicated that the features in the central front played a role for the propagation of fractures which eventually led to calving. We designed calving Scenario I to follow a similar path in the central ice shelf front. A later calving event in 2008 was delineated by crevasses propagating from Bawden Ice Rise towards the centre of the ice shelf; thus a combination of the 1986 and 2008 calving events would resemble Scenario II. However, if the calving occurred within the next few years, the calving front position would retreat 30 km further upstream compared to 1986.

3.2 Stress field development

To investigate the impact of the two calving scenarios on ice shelf stability, we present fields of the difference between the predicted directions of ice flow and of first principal stress (the *stress-flow angle*; Fig. 3). This diagnostic has previously been used to investigate ice shelf stability on the basis that existing weaknesses (rifts and crevasses) are typically oriented across-flow (Kulessa et al., 2014). Regions of the shelf exhibiting low stress-flow angles are likely to be more affected by small-scale calving because stresses act to open existing weaknesses; conversely, regions with a stress-flow angle approaching 90° are likely to be stable.

The stress-flow angles at the present (early 2015) ice front are generally high (Fig. 3a) and, as a result, calving events are rare and the ice front is stable (Kulessa et al., 2014). If the ice shelf calves under Scenario I, the new ice front will, in the immediate term, still mostly be fringed by ice with a high stress-flow angle (Fig. 3a). However, this safety margin is narrowed by the calving, and the centre of the new ice front will exhibit very low stress-flow angles. Under this modest calving scenario, if the ice shelf is able to adapt to the new geometry (Fig. 3b), a new region of high stress-flow angles develops, but this region remains significantly narrower than at present. Under calving Scenario II, much more of the ice front is immediately left without a buffer of high stress-flow angle ice (Fig. 3a). Even if it were possible to adapt to this new geometry (Fig. 3c), a significant section of the new ice front would retain very low values of stress-flow angle.

An alternative measure of stability was presented by Doake et al. (1998), whereby ice downstream of a "compressive arch" represented by a contour of zero second principle stress is subject to purely tensile stresses and regarded as a

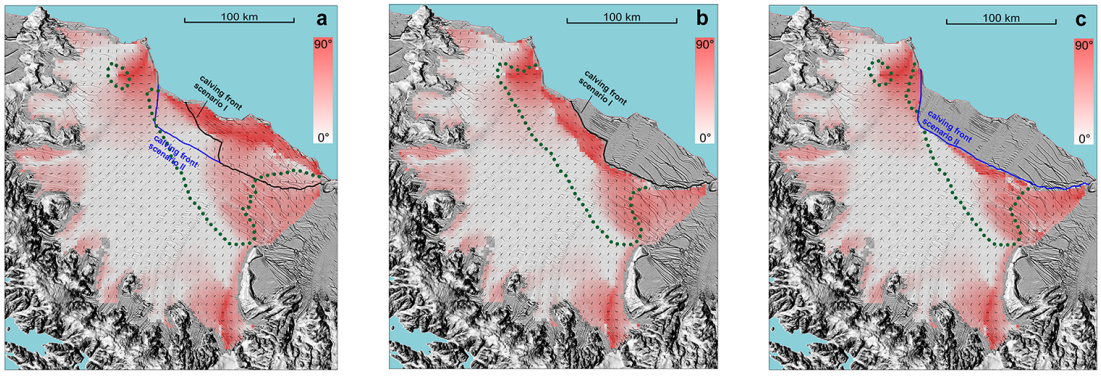

Figure 3. Results from ice shelf flow model: stress-flow angle fields for the present-day ice front geometry **(a)** and for the new geometries under Scenarios I **(b)** and II **(c)**. The green dotted line represents the contour line of zero second principal stress.

passive part of the ice shelf, its presence indicating a stable front. This is a more conservative measure of stability than the stress-flow angle and we include it for completeness. The dotted line in all panels of Fig. 3 represents the zero second principal stress contour line for the reference simulation and the two new calving fronts. For Scenario I this line is breached by the new calving front in the south at the Gipps Ice Rise; for Scenario II it is breached on both sides.

4 Discussion

The rift highlighted here has been present since the earliest satellite imagery (Glasser et al., 2009) but has recently propagated beyond its neighbouring structures to the point at which a large calving event is anticipated. Over the past 4 years the rate of development of the rift width has been steady, but the length has grown intermittently with a particular acceleration during 2014 (Fig. 2). We hypothesize that the strain which opens the rift may be relatively constant, but that the fracture response varies with tip position. This may be a result of variations in fracture toughness of the ice which are likely to be related the presence of marine ice in suture zones (Holland et al., 2009; Jansen et al., 2013) and the locations of pre-existing weaknesses. The mean rate of rift propagation appears to be smaller when the rift tip is within a suture zone (Fig. 2).

Further downstream of the current rift another feature is visible which has a similar shape (Figs. 1, 2). We assume that this feature, which is already present in a Landsat image from 1988, is most likely a surface expression of a basal crevasse (Supplement Fig. S1, compare features described in Luckman et al., 2012). It is isolated from the neighbouring flow units. In contrast, the recently propagated rift is an open fracture, widening towards the south, and crossing the Joerg Peninsula suture zone.

The similar shape indicates that both features are initiated in a similar stress environment. In 1988 the isolated basal crevasse was located approximately 10 km downstream of the position of the current rift. The currently active rift is unique due to its connection to the wide rift reaching towards Gipps Ice Rise.

The reduction in area of Larsen C Ice Shelf under Scenarios I and II of 9 and 12 % respectively will be significant, but will of course not contribute to immediate sea level rise since the floating ice already displaces its own weight of seawater. The predicted ice loss is also not unprecedented: in the late 1980s a calving event removed 14 % of Larsen C Ice Shelf (Cook and Vaughan, 2010). The real significance of this new rift to this ice shelf is two-fold. First, the predicted calving will reduce its area to a new minimum both in terms of direct observations, and probably since the last interglacial period (Hodgson et al., 2006). Second, unlike during the 1980s, but highly comparable to the development of Larsen B Ice Shelf between 1995 and 2002, the resulting geometry may be unstable. According to the stress-flow angle criterion, our calving scenarios lead to a range of unstable outcomes from partial to significant. Under our modest rift propagation Scenario I, immediately following the predicted calving event, the central part of the ice front will be unstable and prone to persistent calving of small ice blocks as the principal strain works to open existing fractures. It is not clear how quickly the velocity of a real ice shelf will be able to adapt to the new boundary conditions, but even if this is rapid, the margin of stabilizing ice becomes very narrow. Under Scenario II, the unstable part of the new ice front is considerably larger and, even if the flow field adapts quickly to the new geometry, parts of the calving margin remain unstable and prone to run-away calving of a similar nature to Larsen B Ice Shelf between 1995 and 2002. Assessing the stress field according to Doake et al. (1998), Scenario II would also be considered as an unstable calving front.

Our model demonstrates that the newly developing rift presents a considerable risk to the stability of the Larsen C Ice Shelf.

5 Conclusions

We have investigated a newly developing rift in the south of Larsen C Ice Shelf which has propagated beyond its neighbours in 2013, and grew very rapidly in 2014. It seems inevitable that this rift will lead to a major calving event which will remove between 9 % and 12 % of the ice shelf area and leave the ice front at its most retreated observed position. More significantly, our model shows that the remaining ice may be unstable. The Larsen C Ice Shelf may be following the example of its previous neighbour, Larsen B, which collapsed in 2002 following similar events.

The Supplement related to this article is available online at doi:10.5194/tc-9-1223-2015-supplement.

Acknowledgements. The authors would like to thank Ted Scambos, Catherine Walker and Maurice Pelto for their constructive comments, which helped to improve this manuscript. This work was carried out as part of the MIDAS project funded by NERC (NE/L005409/1) and continues work carried out under the NERC SOLIS project (NE/E012914/1). D. Jansen was funded by the HGF junior research group "The effect of deformation mechanism for ice sheet dynamics" (VHNG 802). We are indebted to NASA for the MODIS and Landsat data. D. Jansen would like to thank C. Wesche for helpful discussions.

Edited by: M. van den Broeke

References

Borstad, C. P., Rignot, E., Mouginot, J., and Schodlok, M. P.: Creep deformation and buttressing capacity of damaged ice shelves: theory and application to Larsen C ice shelf, The Cryosphere, 7, 1931–1947, doi:10.5194/tc-7-1931-2013, 2013.

Cook, A. J. and Vaughan, D. G.: Overview of areal changes of the ice shelves on the Antarctic Peninsula over the past 50 years, The Cryosphere, 4, 77–98, doi:10.5194/tc-4-77-2010, 2010.

Cook, A. J., Murray, T. I., Luckman, A., Vaughan, D. G., and Barrand, N. E.: Antarctic Peninsula 100 m Digital Elevation Model Derived from ASTER GDEM. Boulder, Colorado USA: National Snow and Ice Data Center, doi:10.7265/N58K7711, 2012.

Doake, C. S. M., Corr, H. F. J., Rott, H., Skvarca, P., and Young, N. W.: Breakup and conditions for stability of the northern Larsen Ice Shelf, Antarctica, Nature, 391, 778–780, 1998.

Glasser, N. F., Kulessa, B., Luckman, A., Jansen, D., King, E. C., Sammonds, P. R., Scambos, T. A., and Jezek, K. C.: Surface structure and stability of the Larsen C Ice Shelf, Antarctic Peninsula, J. Glaciol., 55, 400–410, doi:10.3189/002214309788816597, 2009.

Hodgson, D. A., Bentley, M. J., Roberts, S. J., Smith, J. A., Sugden, D. E., and Domack, E. W.: Examining Holocene stability of AntarcticPeninsula ice shelves, Eos Trans. AGU 87, 305–308, doi:10.1029/2006eo310001, 2006.

Holland, P. R., Corr, H. F. J., Vaughan, D. G., Jenkins, A., and Skvarca, P.: Marine ice in Larsen Ice Shelf, Geophys. Res. Lett., 36, L11604, doi:10.1029/2009GL038162, 2009.

Holland, P. R., Corr, H. F. J., Pritchard, H. D., Vaughan, D. G., Arthern, R. J., Jenkins, A., and Tedesco, M.: The air content of Larsen Ice Shelf, Geophys. Res. Lett., 38, L10503, doi:10.1029/2011GL047245, 2011.

Holland, P. R., Brisbourne, A., Corr, H. F. J., McGrath, D., Purdon, K., Paden, J., Fricker, H. A., Paolo, F. S., and Fleming, A. H.: Atmospheric and oceanic forcing of Larsen C Ice Shelf thinning, The Cryosphere Discuss., 9, 251–299, doi:10.5194/tcd-9-251-2015, 2015

Jansen, D., Kulessa, B., Sammonds, P. R., Luckman, A., King, E. C., and Glasser, N. F.: Present stability of the Larsen C Ice Shelf, Antarctic Peninsula, J. Glaciol., 56, 593–600, 2010.

Jansen, D., Luckman, A. J., Kulessa, B., Holland, P. R., and King, E. C.: Marine ice formation in a suture zone on the Larsen C Ice Shelf and its influence on ice shelf dynamics, J. Geophys. Res.-Earth Surf., 118, 1–13, doi:10.10002/jgrf.20120, 2013.

Khazendar, A., Rignot, E., and Larour, E.: Acceleration and spatial rheology of Larsen C Ice Shelf, Antarctic Peninsula, Geophys. Res. Lett., 38, L09502, doi:10.1029/2011GL046775, 2011.

Kulessa, B., Jansen, D., Luckman, A. J., King, E. C., and Sammonds, P. R.: Marine ice regulates the future stability of a large Antarctic ice shelf, Nature Comm., doi:10.1038/ncomms4707, 2014.

Luckman, A., Jansen, D., Kulessa, B., King, E. C., Sammonds, P., and Benn, D. I.: Basal crevasses in Larsen C Ice Shelf and implications for their global abundance, The Cryosphere, 6, 113–123, doi:10.5194/tc-6-113-2012, 2012.

Luckman, A. J., Elvidge, A., Jansen, D., Kulessa, B., Kuipers-Munneke, P., and King, J.: Surface melt and ponding on Larsen C Ice Shelf and the impact of föhn winds, Antarct. Sci., 26, 625–635, doi:10.1017/S0954102014000339, 2014.

McGrath, D., Steffen,K., Holland, P. R., Scambos, T. S., Rajaram, H., Abdalati, W., and Rignot, E.: The structure and effect of suture zones in the Larsen C Ice Shelf, Antarctica, J. Geophys. Res.-Earth Surf., 119, 588–602, doi:10.1002/2013JF002935, 2014.

Pritchard, H. D., Ligtenberg, S. R. M., Fricker, H. A., Vaughan, D. G., van den Broeke, M. R., and Padman, L.: Antarctic ice-sheet loss driven by basal melting of ice shelves. Nature, 484, 502–505, 2012.

Sandhäger, H., Rack, W., and Jansen, D.: Model investigations of Larsen B Ice Shelf dynamics prior to the breakup. Forum for Research into Ice Shelf Processes (FRISP), Report, 16, 5–12, Bjerknes Cent. For Clim. Res., Bergen, Norway, 2005.

Shepherd, A., Wingham, D., Payne, T., and Skvarca, P.: Larsen Ice Shelf has progressively thinned, Science, 302, 856–859, 2003.

van den Broeke, M.: Strong surface melting preceded collapse of Antarctic Peninsula ice shelf, Geophys. Res. Lett., 32, L12815, doi:10.1029/2005GL023247, 2005.